European Archives of Oto-Rhino-Laryngology (2019) 276:3443–3452
https://doi.org/10.1007/s00405-019-05600-8

HEAD AND NECK

Effects of pentoxifylline and tocopherol on a rat-irradiated jaw model using micro-CT cortical bone analysis

Truc Thi Hoang Nguyen[1] · Mi Young Eo[1] · Mi Hyun Seo[1] · Hoon Myoung[1] · Soung Min Kim[1] · Jong Ho Lee[1]

Received: 27 May 2019 / Accepted: 8 August 2019 / Published online: 14 August 2019

Abstract

Purpose A combination of pentoxifylline (PTX) and tocopherol (TP) is believed to reduce chronic fibrosis and induce bone healing in osteoradionecrosis (ORN) of the mandible, but evidence of its therapeutic effectiveness for cortical bone is lacking. This study was designed to determine the effect of combined PTX and TP (PTX + TP) on mandibular cortical bone remodeling in a rat model of ORN, using micro-CT and histological analysis.

Methods Forty-eight 8-week-old male Sprague–Dawley rats were randomly divided into irradiated ($n = 40$) and non-irradiated ($n = 8$) groups. Animals in the irradiated group were divided into four sub-groups, including PTX, TP, PTX + TP, and normal saline. Three weeks after irradiation, mandibular posterior tooth extraction was performed, and animals were sacrificed 7 weeks after irradiation. The mandibles were analyzed using micro-CT and histological evaluation.

Results The alveolar bone height, cortical bone thickness, cortical bone volume, and total cortical bone surface of the PTX + TP group were significantly greater than those of other irradiated groups ($p < 0.05$). In 3D reconstructed images, the residual volumes of cortical and cancellous bone were inadequate in the irradiated groups.

Conclusion We found that a combination of PTX and TP improved quality and quantity of cortical bone in irradiated rat mandibles, thus providing supporting evidence of its utility as a treatment and prophylactic agent in ORN. We observed inadequate volumes of cortical and cancellous bone in ORN mandibles, suggesting that cortical bone could play an important role in further ORN studies.

Keywords Osteoradionecrosis · Pentoxifylline (PTX) · Tocopherol (TP) · Micro-CT · Cortical bone of jaw

Introduction

The use of radiotherapy (RT) in the treatment of head and neck malignancies includes primary therapy, palliative treatment for late stage, and unresectable tumors, adjuvant to surgery and in combination with chemotherapy [1]. With recent advances in radiation techniques, the undesired effects of irradiation have been localized. However, patients still suffer from reactions of the mucosa, jawbone, or salivary glands, among which one specific adverse effect is osteoradionecrosis (ORN) of the mandible [2–4]. ORN is clinically defined by exposed irradiated bone that fails to heal for at least 2 months with the presence of necrotic or devitalized bone and with no evidence of residual or recurrent tumor, as described by Beumer et al. [2]. The influences and sequelae of ORN are pain, difficulties in mastication, and facial deformities if the lesion is neglected [5].

✉ Soung Min Kim
smin5@snu.ac.kr; smin_kim@msn.com

Truc Thi Hoang Nguyen
hoangtruc.bamboo@gmail.com

Mi Young Eo
myoungh@snu.ac.kr

Mi Hyun Seo
mhseo82@hanmail.net

Hoon Myoung
myoungh@snu.ac.kr

Jong Ho Lee
leejongh@snu.ac.kr

[1] Department of Oral and Maxillofacial Surgery, Dental Research Institute, School of Dentistry, Seoul National University, 101 Daehak-ro, Jongno-gu, Seoul 03080, South Korea

The exact pathogenesis of ORN remains a matter of controversy [6, 7]. In 1983, Marx introduced 3H theory, stating that hypoxia, hypovascularity, and hypocellularity collectively cause non-healing wound in ORN [3, 6]. In 2004, Delanian et al. hypothesized that ORN is the result of a radiation-induced fibroatrophic process (RIF) [8] that includes free radical formation, which leads to endothelial dysfunction, inflammation, microvascular thrombosis, fibrosis, and remodeling, and finally results in bone and tissue necrosis [6, 9]. Delanian and colleagues then developed an etiological treatment therapy, which is a combination of antioxidant agents that works via the inhibition of free radical species. In a phase II trial performed by Delanian et al., the combination of pentoxifylline and tocopherol was effective for ORN treatment and led to disease regression [8]. Pentoxifylline (PTX) and tocopherol (TP) together work as potent antifibrotic and antioxidant agents, and are believed to have the combined effect of reducing chronic fibrosis and inducing bone healing in ORN-affected mandibles.[8, 10].

The effects of irradiation on bone composition have been studied in the few past decades, since the disease was first reported. However, the mechanisms underlying ORN remain undefined and the importance of cortical bone remodeling has not been emphasized. Several animal models involving maxillary and mandibular tooth extraction were previously created to study ORN. A review by Fan et al. regarding animal models for treatment of ORN reported the clinical and radiological features of ORN, but few data are available regarding histopathologic findings of irradiated bone in human or experimental studies. The authors suggested that an animal model would be valuable for evaluating the histopathologic findings of irradiated bone, as well as treatments for ORN with tissue engineering biomaterials [11]. However, most previous studies used histologic examinations of specimens as the only evaluation tool. During screening and treatment of ORN patients, some noticeable differences in the destruction of cortical bone and cancellous bone have been observed. The pattern of defects, in that cortical bone has fewer defects than cancellous bone, is different from those of other types of osteomyelitis. Based on these observations, we hypothesize that there are significant differences in necrosis and destruction between irradiated mandibular cortical and cancellous bone and that cortical bone can play an important role in the clinical evaluation and prognosis of ORN.

Micro-CT has exhibited many outstanding features and quickly become a standard tool for the scanning and analysis of bone structure. With the help of this modality and visualized, reconstructed, measurement, and analysis software, it is now possible to accurately visualize bone structure in three dimensions, along with numerous bone structural parameters [12]. However, micro-CT scans must be well-formatted to be able to perform normalized selection of a volume of interest (VOI) for the evaluation of complex bone defects [13]. Protocols for studying cortical bone remodeling in rodent ORN mandibles are particularly scarce and the available methodology is not sufficiently informative [12].

The goal of this study is to assess improvement in cortical bone quality and quantity in an irradiated rat model treated with PTX and TP. This study was designed to improve and update the previous animal models of ORN by including the irradiation of rat mandibles with a targeted device, mandibular molar extraction, and micro-CT, and histological analyses for outcome evaluation. We discuss these updates in the context of evaluating ORN pathologies and present a review of management trends.

Materials and methods

Animal preparation

The study was started with animal preparation and grouping. Forty-eight 8-week-old male Sprague–Dawley rats (OrientBio Inc., Seongnam, Korea) with an average body weight of 369.6 g were used in this study. The study procedures were approved by the Seoul National University Institutional Animal Care and Use Committee (SNU-180213-1-1). The rats were housed in the Laboratory Animal Center of the Korea Institute of Radiological and Medical Sciences in ventilated cages, with standard 12-h light/dark cycles and access to chow and water ad libitum. The rats were randomly divided into an irradiated group (40 rats) and a non-irradiated or control group (8 rats). In the irradiated group, the rats were further divided into four small groups according to medication: PTX, TP, combination of PTX and TP (PTX + TP), and normal saline (NS). Four animals in the irradiated group died and one animal was released from anesthesia during irradiation and was excluded from the study (Table 1).

Table 1 Animal grouping

Medication	N^a
Irradiated groups	
Pentoxifylline (PTX)	10 (1)
Tocopherol (TP)	10 (3)
Pentoxifylline + tocopherol (PTX + TP)	10
Normal saline	10 (1)
Non-irradiated group (C)	8

[a]Four animals died after radiation and one animal was released from anesthesia during irradiation

Irradiation procedures

Irradiation was performed under anesthesia with an intraperitoneal injection of a mixture of ketamine (60 mg/kg) and xylazine (3 mg/kg). The external radiation procedures were performed with an X-RAD 320 Irradiator® (Precision X-ray Inc., North Branford, CT, USA). The irradiator provides a high output uniform beam with a 320-kV X-ray tube. The single radiation dose was 35 Gy and the dose rate was 2.5 Gy/min. The animals were positioned on their right side, and the irradiated area was defined as a 1 × 2 cm rectangle on the left mandibular body with the isocenter located using laser light.

Medicine delivery and extraction procedures

The day after irradiation, drug delivery was initiated. PTX was administered daily at a dose of 50 mg/kg and TP at a dose of 40 IU/kg daily, by oral gavage. All rats underwent atraumatic extraction of the first and the second left mandibular molars under general anesthesia 3 weeks after irradiation. The animals were sacrificed 7 weeks after irradiation and 4 weeks after extraction by CO_2 inhalation. The mandible was isolated, all soft tissue was removed, and then, the mandibular bone was fixed in formalin.

Micro-CT scanning and data reconstruction procedure

Micro-CT was performed using a high-resolution micro-CT scanner Skyscan 1172® (Bruker Co., Kontich, Belgium). The scan parameters were 70 kV, 141 µA, with a 0.5-mm Al filter, undergoing a 360° rotation with 0.4° steps. The data sets were reconstructed with NRecon software® (SkyScan Co., Aartselaar, Belgium) with adjusted beam-hardening factor correction, ring artifact reduction, and smoothing. Quantitative information regarding bone structure was assessed using a data viewer and the CtAn Image Processing Language® (Bruker Co., Kontich, Belgium).

Definition of the region of interest (ROI) and volume of interest (VOI)

The VOI included the entire defect volume in the first and second molar region post-extractions, with a fixed data set of 360 slices. The ROI was defined as the entirety of the cortical bone and was managed semi-manually. After manual delineation matching the cortical bone area, the ROIs were then interpolated for the next slices and were continuously checked and re-delineated to ensure that no cortical bone was cropped out.

Cortical bone parameter assessment

The cortical bone-related parameters, including the total cortical bone volume (Ct.BV, mm^3), CBT (Ct.Th, mm), cortical bone surface (Ct.S, mm^2), total volume of pore space (Po.V, mm^3), and the rate of porosity (PoV%) were measured and recorded. Three-dimensional (3D) images of mandibular bony defects were reconstructed with CTVol software® (SkyscanVR, Kontich, Belgium).

In the Dataview window, one slice, which was located in the middle of the first molar tooth, was chosen (Fig. 1). The alveolar bone height (ABH) and cortical bone thickness (CBT) on both the buccal and lingual side of the extracted and non-extracted jaw were assessed and measured using CTAn® and ImageJ® (Bethesda, MD, USA).

Histological and immunohistochemical evaluation

Decalcified paraffin-embedded tissues were sectioned at 4-µm intervals and collected in serial sections on slide glass for both H&E and immunohistochemical staining with an automated BOND-MAX system® (Leica Microsystems, Mannheim, Germany). The slides were examined using a BX41® Light Microscope (Olympus Co., Tokyo, Japan). The IHC markers used include TNF-α, TGF-β1, IL-6, ALP, osteocalcin (OC), and CD31. For the evaluation of microvessel density (MVD), slides were scanned and "hot spots" were identified at 40× magnification. The number of $CD31^+$ microvessels was counted at 200× magnification per measurement field [14]. Counting was performed in two different fields of cortical bone. OC staining was also screened for osteocytes at 400× magnification. For other antibodies, staining was scored as follows: negative, weak (1–10% of cells positive), moderate (11–50%), and strong (> 50%).

Statistical considerations

Means and standard deviations (SDs) of alveolar bone loss, CBT, and other cortical bone parameters were calculated. The Shapiro–Wilk test was used to assess the normality of variables and the differences were tested by ANOVA. All analyses were carried out using SPSS 25.0® (SPSS Software Company, Chicago, USA). p values < 0.05 were considered statistically significant.

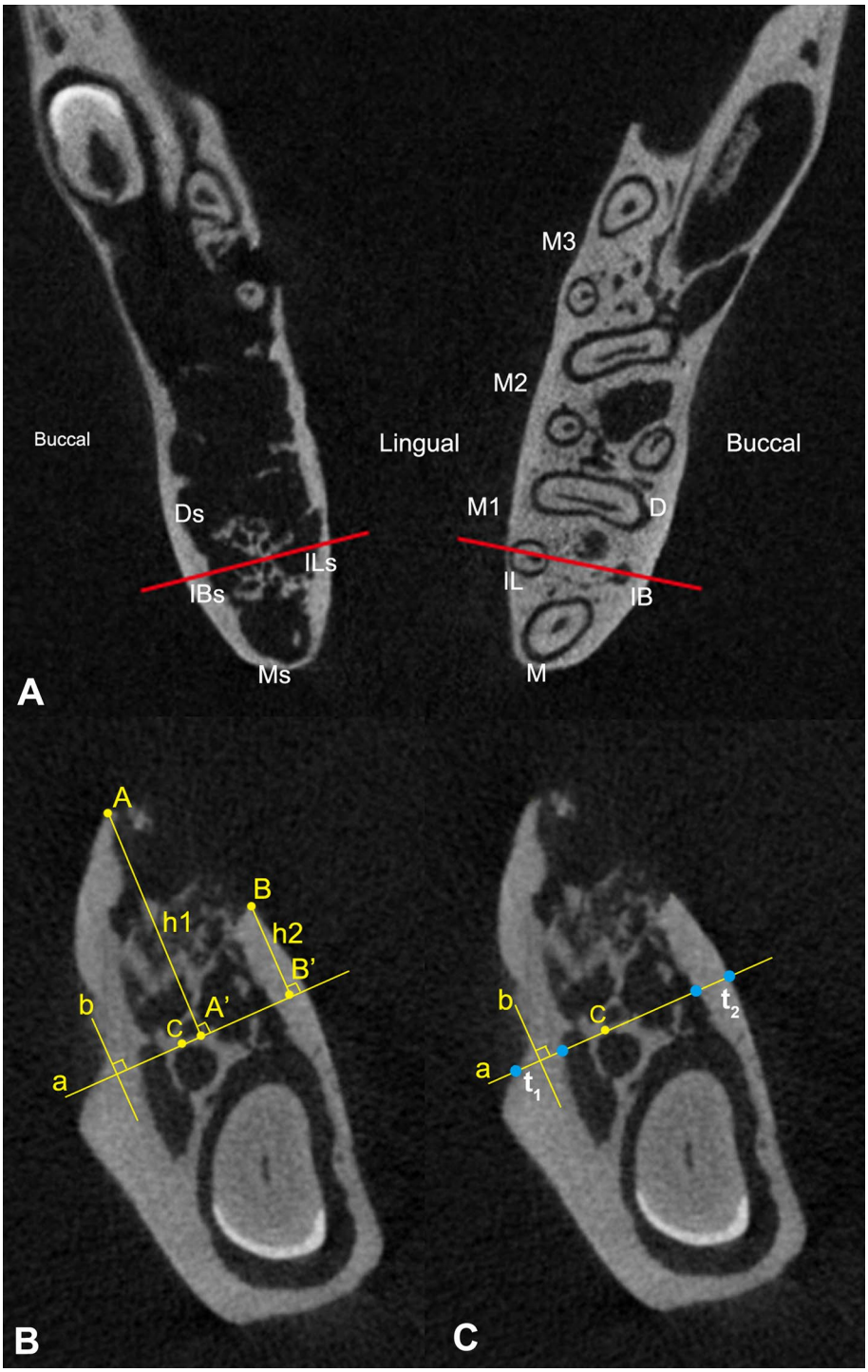

Fig. 1 **a** Selection of one slice using for ABH and CBT measurement, *M1* the first molar, *M2* the second molar, *M3* the third molar, *D* distal root, *M* mesial root, *IL* intermediate lingual root, *IB* intermediate buccal root, *Ds, ILs, IBs, Ms* the socket of corresponding tooth roots on the extracted site. **b** ABH measurement method (a) is the line drawn tangential to the upper cortical border of the mandibular canal at C and perpendicular to the external surface of the buccal plate (b), A point is top of the vestibular crest, A′ point is the point of intersection of line draw from A and perpendicular to (a), B point is top of the lingual crest, B′ point is the point of intersection of line draw from B and perpendicular to (a), *h*1, *h*2 is the cortical bone height on vestibular and lingual side, respectively, **c** CBT measurement method, t1 is CBT of buccal wall, t2 is CBT of lingual wall

Results

We observed areas of depilation in irradiated mandibles, and other alterations of teeth were also recorded, including stopped growth of mandibular incisors and dental fractures, which were observed in three animals. Non-healing mucosal wounds were observed at the extraction zone in irradiated mandibles.

ABH and CBT evaluation

ABHs and CBTs were compared between non-irradiated and NS groups (Table 2). Both ABH and CBT results in NS were significantly lower than the ABH and CBT in the non-irradiated group. In irradiated groups, ABH and CBT of the PTX + TP group were significantly higher than in the other groups. The ABH and CBT of the PTX and TP groups did

Table 2 Comparison of the ABH and CBT on the extracted mandibles between non-irradiated (C) and NS groups

	Buccal side	Lingual side
ABH (mm)		
C	3.87 ± 0.14	1.75 ± 0.14
NS	2.72 ± 0.16	0.97 ± 0.20
CBT (mm)		
C	0.45 ± 0.07	0.31 ± 0.10
NS	0.25 ± 0.11	0.17 ± 0.09

The ABH and CBT in the NS group were significantly lower than ABH and CBT in the non-irradiation group

not significantly differ (Tables 3, 4). The CBT of the PTX group was significantly higher than that of the NS group ($p < 0.05$) (Table 4).

Alveolar bone loss was defined as the difference in ABH between the irradiated jaw and opposite jaw and designated as ΔHB and ΔHL for the buccal side and lingual side, respectively (Table 3). In all irradiated groups, ΔHL results were significantly higher than ΔHB. In addition, on the buccal side, the ΔHB of PTX + TP group was significantly lower compared to the PTX and NS group. On the lingual side, the ΔHL of the NS group was significantly higher than the ΔHL of the PTX and PTX + TP groups ($p < 0.05$).

Cortical bone parameter analysis

In the irradiated group, Ct.BV and total Ct.S of the PTX + TP group were significantly higher than those of the PTX, TP and NS groups (Table 5). The average Ct.Th of the PTX + TP group was significantly higher than that of the NS group. The PoV of the four groups did not differ significantly. However, the total pore volume rate (PoV%) in the PTX + TP group was significantly lower than that of the PTX and NS groups and did not significantly differ from that of the TP group ($p < 0.05$).

3D-reconstructed image evaluation

Cortical bone defects were evaluated using 3D-reconstructed images (Fig. 2). In all four irradiated groups, lingual wall defects were relatively more severe than the buccal wall defection. In addition, defects were smaller in the PTX + TP group than that in the PTX, TP, and NS groups. 3D-reconstructed images were also used to evaluate the relationships between cortical bone defects and cancellous bone defects at the extracted sites. In the irradiated groups, non-healing wounds and bone necrosis were observed. In addition, in the irradiated groups, the residual volumes of cortical bone and cancellous bone were inadequate. 3D reconstruction of intracortical bone porosity and vessel canals showed higher bone vascularity in PTX + TP groups (Fig. 2).

Histological and immunohistochemical findings

We observed empty lacunae with loss of nuclei in the irradiated groups, especially in the NS group. Viable blood vessels within Haversian canals were observed in the PTX + TP group, and to a smaller extent in the PTX group. In the TP and NS groups, unviable blood vessels dominated within Haversian canals (Fig. 3). CD31 staining was used for the evaluation of MVD (Table 6). The MVD of the PTX + TP group was significantly higher

Table 4 Comparison of CBT between irradiation groups:

	Buccal side	Lingual side
CBT (mm)		
PTX	0.32 ± 0.12	0.25 ± 0.06
TP	0.28 ± 0.11	0.18 ± 0.10
PTX + TP	0.42 ± 0.12*	0.30 ± 0.12*
NS	0.25 ± 0.11	0.17 ± 0.09

*The CBT of PTX + TP administrated group was significantly higher than that of other groups

Table 3 Alveolar bone height of each irradiated group

	PTX	TP	PTX + TP	NS
HB1	3.07 ± 0.09	2.90 ± 0.12	3.29 ± 0.20	2.72 ± 0.16
HB2	3.53 ± 0.19	3.41 ± 0.18	3.59 ± 0.14	3.29 ± 0.15
HB2 – HB1 (ΔHB)	0.46 ± 0.12	0.51 ± 0.11	0.29 ± 0.11*	0.58 ± 0.11
HL1	1.20 ± 0.24	1.03 ± 0.20	1.33 ± 0.14	0.97 ± 0.20
HL2	1.76 ± 0.27	1.66 ± 0.18	1.64 ± 0.18	1.69 ± 0.22
HL2 – HL1 (ΔHL)	0.55 ± 0.14	0.63 ± 0.21	0.31 ± 0.16	0.72 ± 0.25**

HB1, *HB2* (*mm*) alveolar bone height (ABH) at the buccal sides of the irradiated jaw and opposite jaw, respectively. *HL1*, *HL2* (*mm*) ABH at the lingual sides of the irradiated jaw and opposite jaw, respectively

*Alveolar bone loss on the buccal side (ΔHB) of the PTX + TP group significantly lower compared to the PTX and NS group

**Alveolar bone loss on the lingual side (ΔHL) of the NS group significantly higher compared to the PTX and PTX + TP groups

Table 5 Cortical bone parameters of the irradiated groups

	PTX	TP	PTX + TP	NS	*p* value
Ct.BV	30.72 ± 1.32	29.71 ± 1.55	33.04 ± 1.88**	29.02 ± 1.12	< 0.03**
Ct.Th	0.54 ± 0.03	0.54 ± 0.03	0.56 ± 0.02	0.51 ± 0.02*	< 0.02*
Ct.S	206.05 ± 13.62	201.75 ± 15.84	226.23 ± 11.96**	207.40 ± 3.87	< 0.03**
PoV	1.40 ± 0.34	1.19 ± 0.22	1.25 ± 0.20	1.47 ± 0.29	
PoV%	4.52 ± 0.56	4.36 ± 0.69	3.53 ± 0.40*	4.66 ± 0.74	< 0.02*

Ct.BV cortical bone volume, mm^3, *Ct.Th* cortical bone thickness, mm, *Ct.S* cortical bone surface, mm^2, *PoV* total volume of pore space, mm^3, *PoV%* percent of pore space on total cortical bone volume, %. Ct.BV of the PTX + TP group is significantly higher than that of PTX, TP, and NS. CtTh of PTX + TP is significantly higher than that of the NS group. Ct.S of PTX + TP is significantly higher than those of the PTX, TP, and NS groups. The PoV of the four groups did not differ significantly. However, the PoV% for the PTX + TP group is significantly lower than that of PTX and NS, and did not significantly differ from the TP group

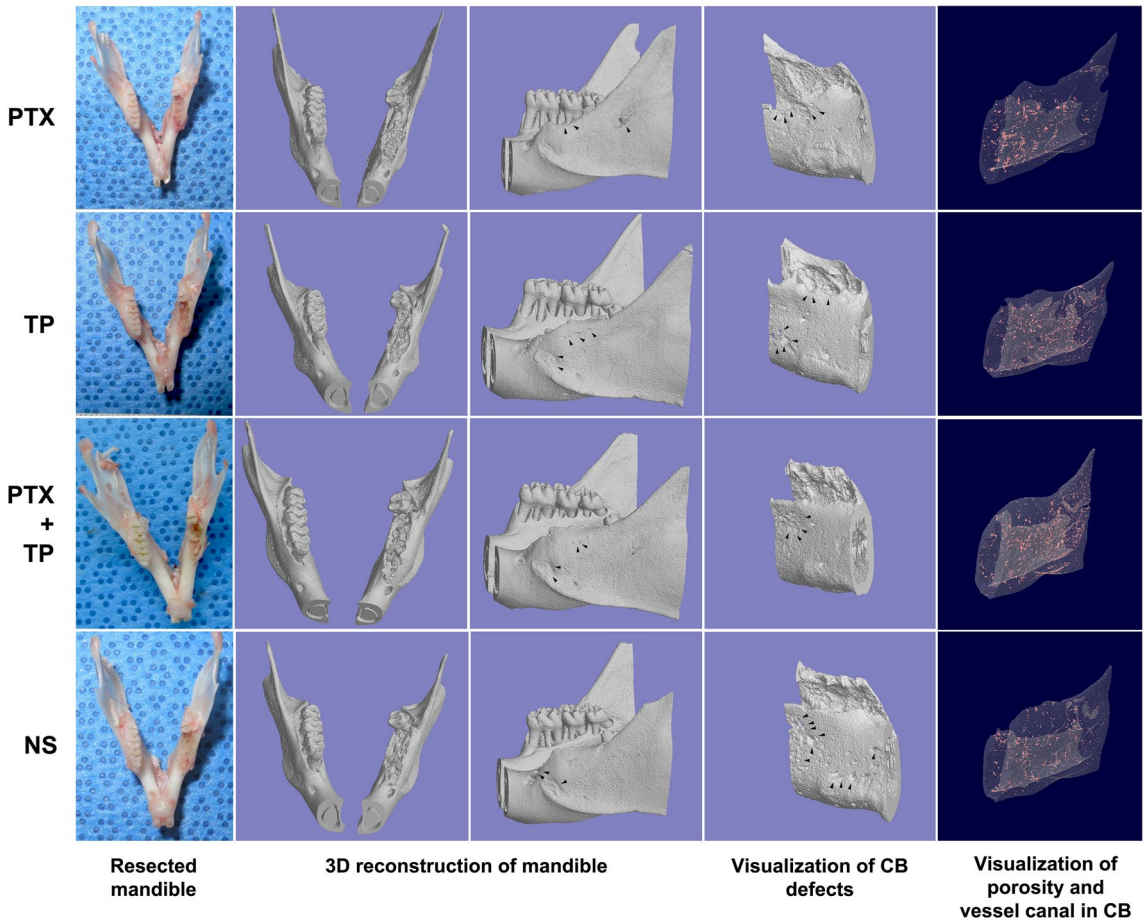

Fig. 2 3D reconstruction of the cortical bone in irradiated groups and 3D visualization of porosities and vessel canals. The arrows mark the bone defection

than that of the PTX, PT, and NS groups ($p < 0.05$). OC staining was used for the evaluation of osteocytes within cortical bone. The number of OC + osteocytes in the NS group was significantly lower than in the other three groups. The number of OC + osteocytes in the PTX + TP, PTX, and TP groups did not differ significantly. The expressions of TNF-α and TGF-β1 were lowest in the PTX + TP group. The other markers, including IL-6 and ALP, did not show significant differences among groups (Fig. 3; Table 6).

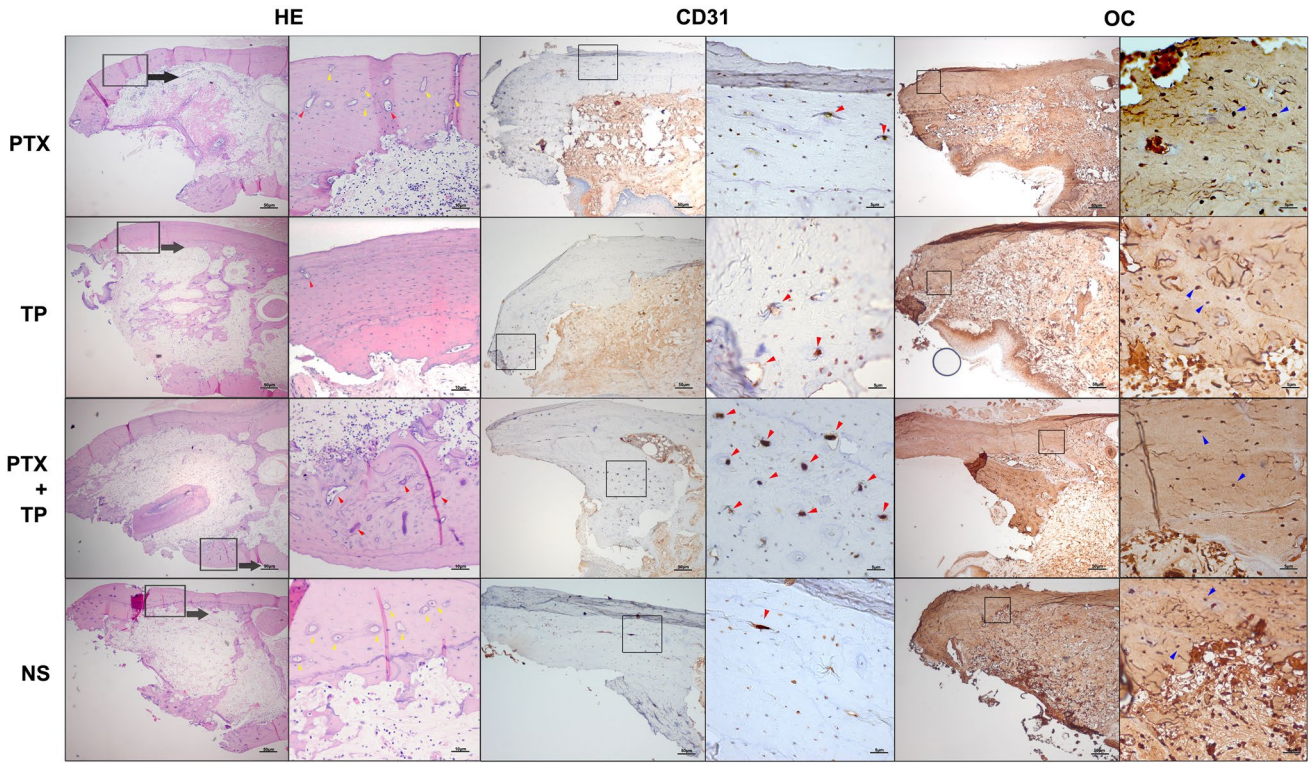

Fig. 3 H&E, CD31, and OC staining in irradiated groups. Red arrows mark viable blood vessels within Haversian canals, and yellow arrows mark unviable blood vessels within Haversian canals. The blue arrows mark OC + osteocytes within cortical bone

Table 6 Microvessel density (MVD) obtained from CD31 staining and immunohistochemical staining score of TNF-α, TGF-β1, ALP, and IL-10 in the four irradiated groups

	MVD	TNF-α		TGF-β1		IL-6		ALP	
		Score 0–1 (%)	Score 2–3 (%)	Score 0–1 (%)	Score 2–3 (%)	Score 0–1 (%)	Score 2–3 (%)	Score 0–1 (%)	Score 2–3 (%)
PTX + TP	15.4 ± 1.4*	88.2	11.8	78.4	21.6	79.3	20.7	52.2	47.8
PTX	10.2 ± 1.2	80.9	20.1	74.9	25.1	80.0	20.0	58.0	42.0
TP	8.0 ± 2.1	70.6	29.4	60.2	9.8	71.5	28.5	61.1	38.9
NS	5.2 ± 1.0	69.2	30.8	60.5	39.5	72	28	60.0	40.0

0: negative, 1: weak (1–10% of cells positive), 2: moderate (11–50% of cells positive), and 3: strong (> 50% of cells positive). MVD in the PTX + TP group was significantly higher than those of the PTX, TP and NS groups (*$p < 0.05$). The expression of TNF-α and TGF-β1 was relatively lower in PTX + TP group. The other markers, including IL6 and ALP, did not show significant differences

Discussion

In this study, micro-CT analysis tools provided repeatable measurements of cortical bone parameters in an animal experiment and also detected morphological changes and ORN manifestation. The ABHs of each jaw were measured on both the buccal and lingual sides. In the non-irradiated group, the ABH of the extracted jaw and the ABH of the opposite jaw on the buccal side and lingual side did not significantly differ between the four groups ($p < 0.05$). In all irradiated groups, the ΔHL were significantly greater than ΔHB. This difference between the treated jaw and non-treated jaw represented cortical bone loss either due to extraction alone or due to the extraction on the irradiated jaw. These results suggest that radiation affects cortical bone; however, the reason why cortical bone loss on the lingual bone wall was greater than on the buccal bone wall remain unclear. We hypothesize that this difference arises because of anatomical factors and the original thickness

of the mandibular bone. The lingual bone wall is usually thinner than the buccal bone wall. Further studies need to be performed to confirm this finding.

Other cortical bone parameters also offer support for treatment using PTX and TP combination. The Ct.BV of the PTX + TP group was significantly higher than those of the PTX, TP, and NS groups. The Ct.Th of the PTX + TP group was significantly higher than of the NS group. The Ct.S of the PTX + TP therapy was significantly higher than of the PTX, TP, and NS groups. The PoV of the four groups did not differ significantly. However, the PoV% in the PTX + TP group was significantly lower than those of other groups. Interestingly, in 3D-reconstructed images, porosity and vessels' canal numbers were higher in PTX + TP groups than in other groups. These results are explained by the total volume of open porosity, which was excluded from intravascular 3D analysis. The low levels of open porosity in PTX + TP groups offer evidence for the bone-healing effect of this combination.

The protocol of this study included irradiation, tooth extraction, and micro-CT and histological analyses. The exact incidence of ORN developing after extraction in irradiated jaws is unknown, but has been reported to range between 2–7% [15, 16]. As tooth extraction is considered one of the main risk factors of ORN, it is useful to include extraction when creating an ORN animal model, thereby defining a reproducible area for micro-CT and histological evaluation. In addition, according to Tamplen et al., when establishing a rat model for ORN, bone metabolism is significantly changed after tooth extraction for 28 days, showing evidence of early ORN manifestation [17]. Therefore, we performed ORN analysis 7 weeks after irradiation (4 weeks after tooth extraction).

In this animal study, we used a single dose of radiation at a rate of 35 Gy, 2.5 Gy/min on a $2 \times 1\text{-cm}^2$ surface of the mandible. According to Hopewell, who detected changes in bone mineral content after singles doses of > 20 Gy, reduction in bony blood flow is dose-related [18]. Niehoff et al. also demonstrated that a single dose of 20 Gy can reduce bone regeneration in rat mandibles [19]. In our study, a single dose of 35 Gy was applied to all irradiated groups, which showed delayed intraoral wound healing and skin alopecia at the irradiated site. In addition, the finding of necrotic bone in micro-CT images of all irradiated groups provides the evidence of radiation-induced osteonecrosis in our animal model.

CD31 is a single-chain type-1 transmembrane protein that plays a role in adhesive interactions between adjacent endothelial cells, as well as between leukocytes and endothelial cells [20]. It has recently been recognized for its angiogenic role [21, 22], and therefore, it was chosen for the MVD analyses in this study. OC and ALP are known to be bone tissue-specific proteins [23] and were used to evaluate cortical bone remodeling. Other markers, including TNF-α, TGF-β1, and IL-6, were used to evaluate inflammation within the cortical bone. As the results have shown, the PTX + TP combination has positive effects on cortical bone angiogenesis and anti-inflammation, as evidenced by the high density of microvessels and osteocytes and the lower expressions of TNF-α and TGF-β1.

During the screening and treatment of ORN patients, some noticeable differences in the destruction of cortical bone and cancellous bone have been observed. In a bisphosphonate-related osteonecrosis of the jaw (BRONJ) patient, both cortical walls exhibited a similar destructive rates as cancellous bone, which resulted in a large defect after saucerization surgery. On the other hand, in a patient with complex ORN defects, the defects appeared on the right and left sides of the mandible, with differences in the general levels of destruction of the cortical and cancellous bone. In another progressive mandibular ORN patient, CT views showed that the rate of destruction of cortical bone was not the same as that of the cancellous bone. After saucerization surgery, a part of the cortical wall showed spontaneous bleeding and vital signs and, therefore, was preserved. Histological images of this patient indicated progress of sclerosis and inflamed internal bone marrow. In an enlarged view of the cortical bone, there were occasional empty lacunae, but lacunae with vital osteocytes dominated, and Haversian canals with vital microvessels were observed. These observations inspire a hypothesis about the defective pattern of ORN that cortical bone has lower defective rates than cancellous bone, unlike other osteomyelitis diseases. Shuster et al. recently revealed difference in pathogenic features between ORN, BRONJ, and bacterial osteomyelitis [24]. The authors concluded that a specific final diagnosis must be made based on patient's history and imaging and cannot be made by microscopic findings alone. Through an animal study, we found that micro-CT is a reliable and promising instrument for distinguishing specific types of osteomyelitis. Further clinical studies, including micro-CT and histological analyses, will be performed to test our hypothesis in terms of distinct destruction patterns of cortical bone in different forms of osteomyelitis.

Our observations and analyses of cortical bone parameters are commensurate with our hypothesis that cortical bone plays an important role in the assessment of ORN pathophysiology and treatment effectiveness. These results can be applied in clinical prognosis and surgical treatment plans. Most importantly, in the treatment of stage II or stage III ORN, cortical bone can be preserved. Instead of total resection, saucerization with necrotic bone removal is recommended, leaving the bleeding cortical bone wall for later bone grafting or a reconstruction. In addition, our findings regarding the therapeutic efficacy of PTX + TP suggest that this combination is applicable for the medical

management of ORN, especially in early stages. PTX + TP can be prescribed as preventive medicine in post-irradiated patients.

PTX is primarily an agent for the treatment of peripheral vascular disease that works by enhancing red blood cell deformability and increasing microcirculation [25]. PTX is also an inhibitor of tumor necrosis factor-alpha (TNF-α), interleukin-1 (IL-1), and fibroblast growth factor (FGF) [26]. Alpha-tocopherol, commonly known as vitamin E, has antioxidant properties [27, 28]. It scavenges reactive oxygen species (ROS) that induce lipid peroxidation in cell membranes and, therefore, protects cell membranes from the oxidative stress induced by radiation [6]. It is also reported to play a role in the reduction of fibrosis and cell apoptosis by its actions on TGF-β1, intercellular adhesion molecular 1 (ICAM-1), and proliferator activated receptor-gamma (PPAR-γ) [26]. Recently, the combination of PTX-TP has been considered a useful protocol for irradiated patients. Delanian et al. reported a reduction of ORN when PTX (800 mg/day) and TP (1000 mg/day) were given for 6 months [29, 30].

Based on recent studies, the cortical bone is considered an important target for bone quality assessment and pharmacological treatment [31]. Bagi et al. [32] suggested that micro-CT imaging of the jawbone is a reliable methodology for the assessment of the cortical bone morphology, microarchitecture, mineral density, and the process of remodeling bone growth into the defect in 2D and 3D planes in a rodent model. Another advantage of the micro-CT technique over histology is that microradiographs can be easily obtained, in a relatively short period of time and at low cost [33].

In summary, our findings demonstrate that the combination of PTX and TP improves the quality and quantity of cortical bone in irradiated rat mandibles, thus supporting its utility as a treatment and prophylaxis agent for ORN. We observed inadequate destruction of cortical and cancellous bone in ORN mandibles, suggesting that cortical bone will play an important role in further ORN studies. In addition, we found that micro-CT is a reliable instrument for mandibular cortical bone assessment and qualification.

Acknowledgements This study was supported by Grant no 03-2019-0043 from the SNUDH Research Fund and by Basic Science Research Program of NRF funded by the Ministry of Education (2017R1D1A1B04029339).

Funding This study had no funding.

Compliance with ethical standards

Conflict of interest There are no conflicts of interest in this article.

Ethical approval The study procedures received the animal research ethics approval from the Seoul National University Institutional Animal Care and Use Committee (SNU-180213-1-1), and with the 1964 Helsinki declaration and its later amendments or comparable ethical standards.

References

1. Madrid C, Abarca M, Bouferrache K (2010) Osteoradionecrosis: an update. Oral Oncol 46(6):471–474
2. Beumer J 3rd, Silverman S Jr, Benak SB Jr (1972) Hard and soft tissue necroses following radiation therapy for oral cancer. J Prosthet Dent 27(6):640–644
3. Marx RE (1983) Osteoradionecrosis: a new concept of its pathophysiology. J Oral Maxillofac Surg 41(5):283–288
4. Coffin F (1983) The incidence and management of osteoradionecrosis of the jaws following head and neck radiotherapy. Br J Radiol 56(671):851–857
5. Thorn JJ, Hansen HS, Specht L, Bastholt L (2000) Osteoradionecrosis of the jaws: clinical characteristics and relation to the field of irradiation. J Oral Maxillofac Surg 58(10):1088–1093 **(discussion 93–5)**
6. Lyons A, Ghazali N (2008) Osteoradionecrosis of the jaws: current understanding of its pathophysiology and treatment. Br J Oral Maxillofac Surg 46(8):653–660
7. Rivero JA, Shamji O, Kolokythas A (2017) Osteoradionecrosis: a review of pathophysiology, prevention and pharmacologic management using pentoxifylline, alpha-tocopherol, and clodronate. Oral Surg Oral Med Oral Pathol Oral Radiol 124(5):464–471
8. Delanian S, Depondt J, Lefaix JL (2005) Major healing of refractory mandible osteoradionecrosis after treatment combining pentoxifylline and tocopherol: a phase II trial. Head Neck 27(2):114–123
9. Delanian S, Lefaix JL (2004) The radiation-induced fibroatrophic process: therapeutic perspective via the antioxidant pathway. Radiother Oncol 73(2):119–131
10. McCaul JA (2014) Pharmacologic modalities in the treatment of osteoradionecrosis of the jaw. Oral Maxillofac Surg Clin N Am 26(2):247–252
11. Fan H, Kim SM, Cho YJ, Eo MY, Lee SK, Woo KM (2014) New approach for the treatment of osteoradionecrosis with pentoxifylline and tocopherol. Biomater Res 18:13
12. Chatterjee M, Faot F, Correa C, Duyck J, Naert I, Vandamme K (2017) A robust methodology for the quantitative assessment of the rat jawbone microstructure. Int J Oral Sci 9(2):87–94
13. Snoeks TJ, Kaijzel EL, Que I, Mol IM, Lowik CW, Dijkstra J (2011) Normalized volume of interest selection and measurement of bone volume in microCT scans. Bone 49(6):1264–1269
14. Wobser M, Siedel C, Kneitz H, Brocker EB, Goebeler M, Houben R et al (2013) Microvessel density and expression of vascular endothelial growth factor and its receptors in different subtypes of primary cutaneous B-cell lymphoma. Acta Derm Venereol 93(6):656–662
15. Nabil S, Samman N (2011) Incidence and prevention of osteoradionecrosis after dental extraction in irradiated patients: a systematic review. Int J Oral Maxillofac Surg 40(3):229–243
16. Kuo TJ, Leung CM, Chang HS, Wu CN, Chen WL, Chen GJ et al (2016) Jaw osteoradionecrosis and dental extraction after head and neck radiotherapy: A nationwide population-based retrospective study in Taiwan. Oral Oncol 56:71–77
17. Tamplen M, Trapp K, Nishimura I, Armin B, Steinberg M, Beumer J et al (2011) Standardized analysis of mandibular osteoradionecrosis in a rat model. Otolaryngol Head Neck Surg 145(3):404–410
18. Hopewell JW (2003) Radiation-therapy effects on bone density. Med Pediatr Oncol 41(3):208–211

19. Niehoff P, Springer IN, Acil Y, Lange A, Marget M, Roldan JC et al (2008) HDR brachytherapy irradiation of the jaw - as a new experimental model of radiogenic bone damage. J Craniomaxillofac Surg 36(4):203–209
20. Pusztaszeri MP, Seelentag W, Bosman FT (2006) Immunohistochemical expression of endothelial markers CD31, CD34, von Willebrand factor, and Fli-1 in normal human tissues. J Histochem Cytochem 54(4):385–395
21. Zhou Z, Christofidou-Solomidou M, Garlanda C, DeLisser HM (1999) Antibody against murine PECAM-1 inhibits tumor angiogenesis in mice. Angiogenesis 3(2):181–188
22. El-Rouby DH (2010) Association of macrophages with angiogenesis in oral verrucous and squamous cell carcinomas. J Oral Pathol Med 39(7):559–564
23. Wei J, Karsenty G (2015) An overview of the metabolic functions of osteocalcin. Rev Endocr Metab Disord 16(2):93–98
24. Shuster A, Reiser V, Trejo L, Ianculovici C, Kleinman S, Kaplan I (2019) Comparison of the histopathological characteristics of osteomyelitis, medication-related osteonecrosis of the jaw, and osteoradionecrosis. Int J Oral Maxillofac Surg 48(1):17–22
25. Ward A, Clissold SP (1987) Pentoxifylline. A review of its pharmacodynamic and pharmacokinetic properties, and its therapeutic efficacy. Drugs 34(1):50–97
26. Pareek P, Samdariya S, Sharma A, Gupta N, Shekhar S, Kirubakaran R (2016) Pentoxifylline and vitamin E alone or in combination for preventing and treating side effects of radiation therapy and concomitant chemoradiotherapy. Cochrane Database Syst Rev 2016(3):CD012117
27. Azzi A, Ricciarelli R, Zingg JM (2002) Non-antioxidant molecular functions of alpha-tocopherol (vitamin E). FEBS Lett 519(1–3):8–10
28. Azzi A, Meydani SN, Meydani M, Zingg JM (2016) The rise, the fall and the renaissance of vitamin E. Arch Biochem Biophys 595:100–108
29. Delanian S, Balla-Mekias S, Lefaix JL (1999) Striking regression of chronic radiotherapy damage in a clinical trial of combined pentoxifylline and tocopherol. J Clin Oncol 17(10):3283–3290
30. Delanian S, Chatel C, Porcher R, Depondt J, Lefaix JL (2011) Complete restoration of refractory mandibular osteoradionecrosis by prolonged treatment with a pentoxifylline-tocopherol-clodronate combination (PENTOCLO): a phase II trial. Int J Radiat Oncol Biol Phys 80(3):832–839
31. Muller R (2009) Hierarchical microimaging of bone structure and function. Nat Rev Rheumatol 5(7):373–381
32. Bagi CM, Moalli MR (2011) Comparative bone anatomy of commonly used laboratory animals: implications for drug discovery. Comp Med 61(1):76–85
33. Schortinghuis J, Ruben JL, Meijer HJA, Bronckers ALJJ, Raghoebar GM, Stegenga B (2003) Microradiography to evaluate bone growth into a rat mandibular defect. Arch Oral Biol 48(2):155–160